EFFECTS OF INITIAL STATIC SHEAR ON CYCLIC RESISTANCE AND PORE WATER GENERATION OF DENSE TOYOURA SAND IN LARGE-STRAIN TORSIONAL SHEAR TESTS

Muhammad UMAR[1], Takashi KIYOTA[2], Nazish ULLAH[3] and Gabriele CHIARO[4]

ABSTRACT:

In this paper, the influence of initial static shear on the deformation characteristics of dense Toyoura sand (D_r ~ 71%) during undrained cyclic shearing is presented. Air pluviated hollow cylindrical specimens were isotopically consolidated and subsequently sheared by using a modified torsional shear device. By using two different combinations of cyclic and static shear stresses, two types of cyclic behavior (i.e. cyclic mobility and residual deformation accumulation) were attained. It was observed that the presence of static shear influenced the effective stress path, shear strain development, and pore water pressure development. Under stress reversal loading conditions, the static shear effects are detrimental leading to the reduction of the cyclic resistance. Whereas, for intermediate stress reversal loading conditions, the effect of initial static shear on cyclic resistance is beneficial.

Key Words: *Initial static shear, Torsional shear, Large strain, Dense sand*

INTRODUCTION

Slope failure is one of the most severe geotechnical disasters induced by earthquakes. Sloping ground conditions on the undrained cyclic behavior of sands have been simulated in laboratory either by conventional triaxial testing (Lee et al., 1967; Vaid et al., 1983; Tatsuoka et al., 1982 Yang and Sze, 2011; among others) or using simple shear conditions (Yoshimi et al., 1975; Vaid et al., 1979; Ishihara and Takatsu, 1977; Vaid et al., 2001; Chiaro et al., 2012 and 2013, Umar et al., 2016 and 2017). The major conclusion from these studies are that the initial static shear stress induced by sloping ground significantly affected cyclic resistance of sandy soils. However, depending on the cyclic shear stress, soil relative density, confining pressure and the mode of deformation (i.e. triaxial vs. simple shear), among other factors, the effect of initial static shear may be beneficial or detrimental. Due to the scarcity of experimental data and the lack of convergence and consistency in the existing data, it has been strongly recommended that experimental findings should not be used by non-specialists or in routine engineering practice (Youd et al., 2001). Clearly, there is a need for continued in-depth research to improve our understanding of the complicated effects of initial static shear on the cyclic resistance of sandy soils within sloping ground.

A soil element beneath the sloped ground is subjected to initial static shear stress (τ_{static}) before an

[1] Project researcher, Institute of industrial science, University of Tokyo
[2] Associate Professor, Institute of Industrial Science, University of Tokyo
[3] Graduate Student, Dept. of Civil Eng. University of Tokyo
[4] Senior Lecturer, Dept. of Civil Eng., University of Canterbury

earthquake, as shown in **Figure 1**. Due to the superimposition of static shear stress (τ_{static}) with cyclic shear stress (τ_{cyclic}), during an earthquake, the soil element may experience stress reversal or stress non-reversal loading conditions.

Precisely, when $\tau_{static} < \tau_{cyclic}$, the shear stress changes during each loading cycle within a maximum positive value ($\tau_{max} = \tau_{static} + \tau_{cyclic} > 0$) to a minimum negative value ($\tau_{min} = \tau_{static} - \tau_{cyclic} < 0$). This type of loading is well known as stress reversal or two-way loading. Whereas, when τ_{static} => τ_{cyclic}, shear stress remains positive (i.e. τ_{max} => 0 and τ_{min} => 0). This is termed stress intermediate, stress non-reversal or one-way loading (Yoshimi and Oh-oka 1975; Hyodo et al. 1991; among others).

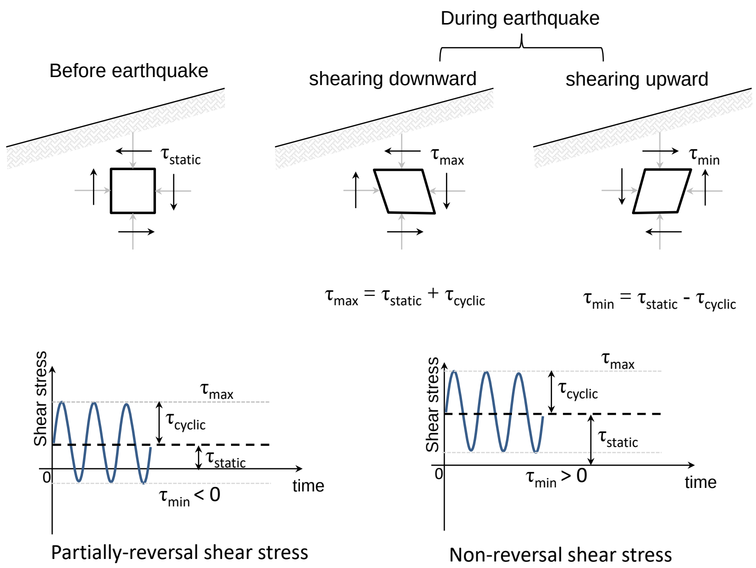

Figure 1. Stress conditions in a sloping ground during an earthquake

Despite extensive research in the past on the importance of initial static shear on undrained cyclic behavior, its effects on the post liquefaction large deformation characteristic lacks complete understanding. Therefore, in this study, the impact of initial static on effective stress path, pore water generation, and large cyclic strain accumulation were investigated, focusing on the case of dense Toyoura sand.

TEST APPARATUS, MATERIAL AND PROCEDURE

Laboratory testing was carried out using the fully automated torsional apparatus (**Figure 2**), which has been developed in the Institute of Industrial Science, University of Tokyo (Kiyota et al., 2008). It can achieve double amplitude shear strain levels of 80% on a hollow cylindrical specimen (height of 20cm, outer diameter 10cm and 6cm). It is operated by using a belt-driven torsional loading system that is connected to an AC servo motor through electromagnetic clutches and a series of reduction gears. Torque moment and axial load are measured by a two-component load cell, which is installed inside the pressure cell. The axial load and torque moment capacities are 8 kN and 0.15 kNm, respectively. The difference in pressure levels between the cell pressure and the pore water pressure are measured by a high-capacity differential pressure transducer (HCDPT) with a capacity of over 600 kPa. A low capacity pressure transducer (LCDPT) is used to measure volume change during consolidation by the difference in water level between two burettes with one collecting water from the specimen and the other as a reference. An external potentiometer with a wire and a pulley is employed to measure the rotation angle of the top cap and, thus, the large torsional deformation. Shear stress amplitude is controlled by a computer, which monitors the outputs from the load cell, computes the corresponding stress value and controls the device accordingly.

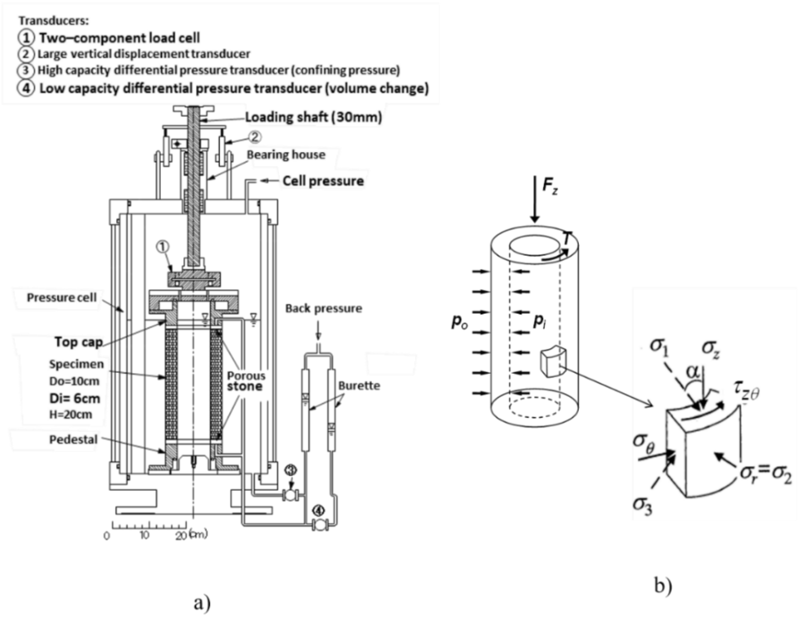

Figure 2. Torsional shear apparatus employed in this study a) Torsional setup b) external forces and stress components action on hollow cylindrical specimen (after Kiyota et al., 2008)

All the experiments were performed on Toyoura sand. The material properties of the Toyoura sand and loading combinations of initial static shear and cyclic shear are listed in Tables 1 and 2, respectively. Air-dried sand particles were poured through a funnel at a constant height to achieve a uniform soil relative density of ~71%. Subsequently, the specimens were consolidated to a mean effective principle stress of 100 kPa with a back pressure of 200 kPa.

In order to replicate the sloping ground conditions, drained monotonic torsional shear stress was applied up to the desired level of static shear stress (Table 2) before applying the cyclic torsional loading in undrained conditions. The loading direction was reversed after reaching the peak shear stress value (corrected for the membrane force, Chiaro et al., 2021) in one direction.

Table 1. Material Properties

Material	Specific Gravity, Gs	Min Void Ratio, e_{min}	Max void ratio e_{max}	Mean Diameter, D_{50} (mm),	Fines Content, FC %
Toyoura Sand	2.659	0.61	0.951	0.20	0.1

Table 2. List of Test Performed

Test	Relative Density, *D*r (%)	Cyclic shear τ_{cyclic} (kPa)	Static shear τ_{static} (kPa)	$\tau_{static} \pm \tau_{cyclic}$ (kPa)	Type of Loading
TEST No 1	71.8	20	0	+20/-20	Reversal
TEST No.2	68.1	20	10	+30/-10	Reversal
TEST No. 3	71.6	20	20	+40/00	Intermediate
TEST No. 4	70.0	30	0	+30/-30	Reversal
TEST No. 5	71.2	30	10	+40/-20	Reversal

TEST RESULTS AND DISCUSSIONS

Correction for membrane force

In torsional shear tests on hollow cylindrical soil specimens, due to the presence of inner and outer membranes, the effect of membrane force on measured torsional shear stress cannot be neglected (Koseki et al. 2005) i.e. to calculate the shear stress effectively applied on the soil specimen, the total stress measured by the load cell needs to be corrected for the apparent shear stress induced by the presence of the membrane.

Usually, the membrane force is computed based on the linear elasticity theory, which assumes a cylindrical deformation of the specimen. Nevertheless, experimental evidence clearly indicates that at large shear strains, the deformation of a hollow cylindrical sand specimen is not uniform along the specimen height, and specimen shape is far from being perfectly cylindrical (Kiyota et al., 2008; Chiaro et al., 2013). To experimentally evaluate the membrane force, a specific testing procedure was developed by Kiyota et al. (2008), which consists of shearing a hollow cylindrical water specimen from small to large shear strain levels in the torsional shear apparatus.

Figure 3 shows the comparison of the result from water specimens tested by Chiaro et al. (2013) having a height of 30 cm, outer diameter of 15 cm and inner diameter of 9 cm and a specimen used in this study (height = 20 cm, outer diameter =10 cm, and inner diameter = 6 cm). The results are compared in terms of shear strain and apparent shear stress. **Figure 3** shows that the membrane force has an insignificant influence on the specimen size and data is scattered along with the proposed correlation by Chiaro et al. (2021). Therefore, the empirical hyperbolic correlation suggested by Chiaro et al. (2021) is valid and was employed in this study to correct the applied shear stress.

The effective mean principal stress was corrected by using the linear expression between the apparent vertical stress due to membranes ($\sigma_v m/3$) and the shear strain (γ) suggested by Chiaro et al. (2021).

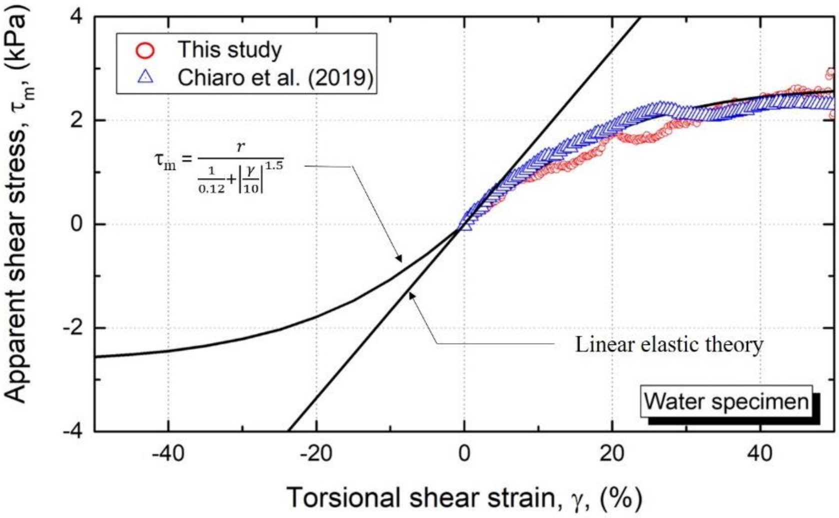

Figure 3. Membrane force correction

Cyclic response of dense sand with static shear

Typical results in terms of effective stress path and stress-strain plot of three undrained cyclic tests subjected to initial static stress ratio ($\alpha = \tau_{static}/p_0'$) of 0, 0.10, and 0.20 consolidated at ≈ 100 kPa and then subjected to a cyclic shear loading under cyclic stress ratio ($CSR = \tau_{cyclic}/p_0' = 0.20$) are presented in **Figure 4, 5** and **6**, respectively. The development of excess pore water pressure (*PWP*) and accumulated shear strains with the increasing number of cycles for α = 0, 0.10, and 0.20 is shown in **Figure 7** and **Figure 8**. All the specimens showed initial contracting behavior characterized by a decrease in the effective stress upon cyclic loading, as shown in **Figure 4(a), 5(a)** and **6(a)**.

As shown in **Figure 7(a) and 7(b)**, in the case of stress reversal loading (CSR > α), the progressive generation of *PWP* besides a nearly zero shear strain development is observed until the state of liquefaction (p' = 0) at Δu =100 kPa is achieved. After the p'-zero state, a sudden development of large shear strain is clearly observed with increasing number of cycles. The number of cycles to reach the state of p'=0 decreased from 33 to11.2 for α = 0 and 0.10, respectively. The type of undrained cyclic response shown in **Figure 4** and **5** could potentially induce large post liquefaction deformations in dense sand within sloping ground during strong earthquakes.

For stress intermediate loading conditions (CSR = α), the behavior is different as compared to that of stress reversal (α = 0 and 0.10). In fact, the specimen did not reach the state of full liquefaction (p'=0) and from the very beginning, the *PWP* development and shear strain accumulation increase at a rather constant rate with increasing number of cycles. Eventually, the large extent of residual deformation brought the specimen to the failure.

By the above discussion, the cyclic behavior in dense sand with static shear can be categories into two distinct types: cyclic mobility for the stress reversal loading (CSR < α) and residual strain accumulation for the stress intermediate loading (CSR = α).

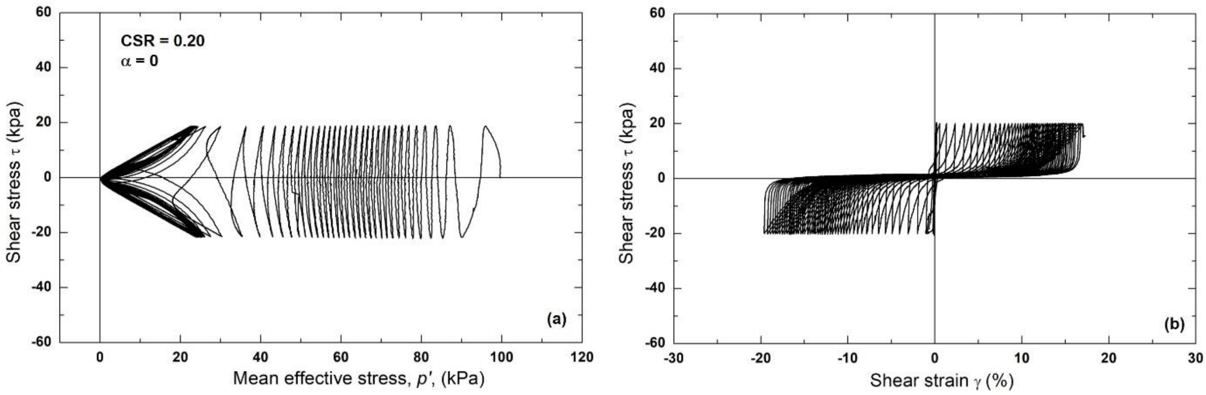

Figure 4. Stress path and stress-strain response of dense Toyoura sand for Test No.1 (D_r = 71.8%, CSR = 0.20, α = 0)

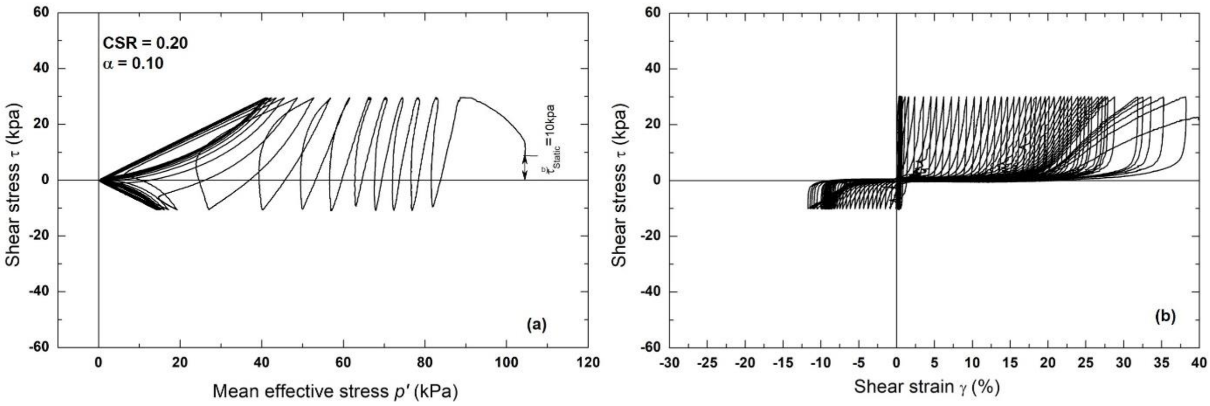

Figure 5. Typical stress path and stress-strain response of dense Toyoura sand for Test No.2 (D_r = 68.1%, *CSR* = 0.20, α = 0.10)

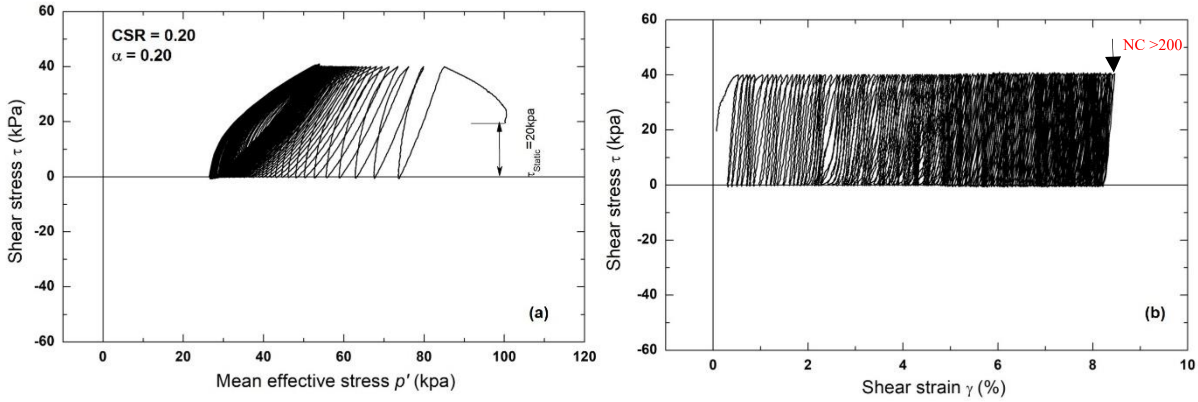

Figure 6. Stress path and stress-strain responses of dense Toyoura sand for Test No.3 (D_r = 71.6%, *CSR* = 0.20, α = 0.20)

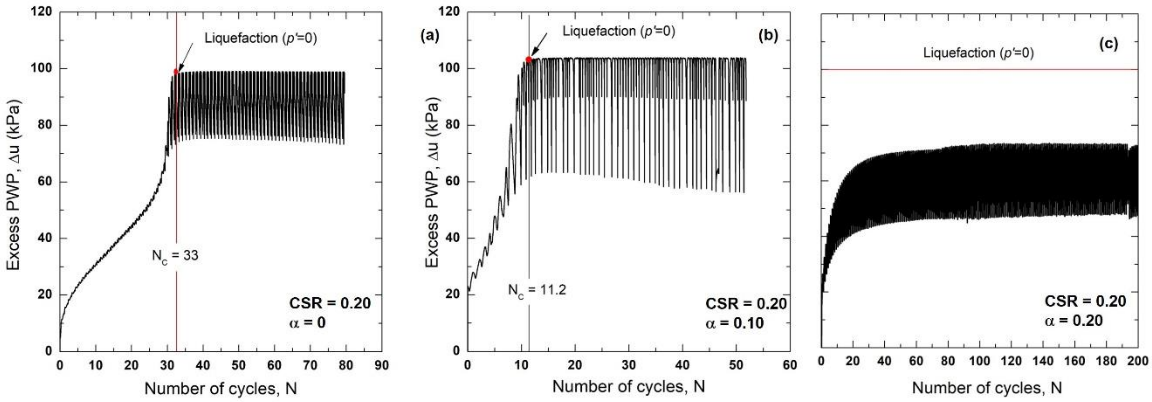

Figure 7. Excess PWP development for *CSR* = 0.20 and varying α values

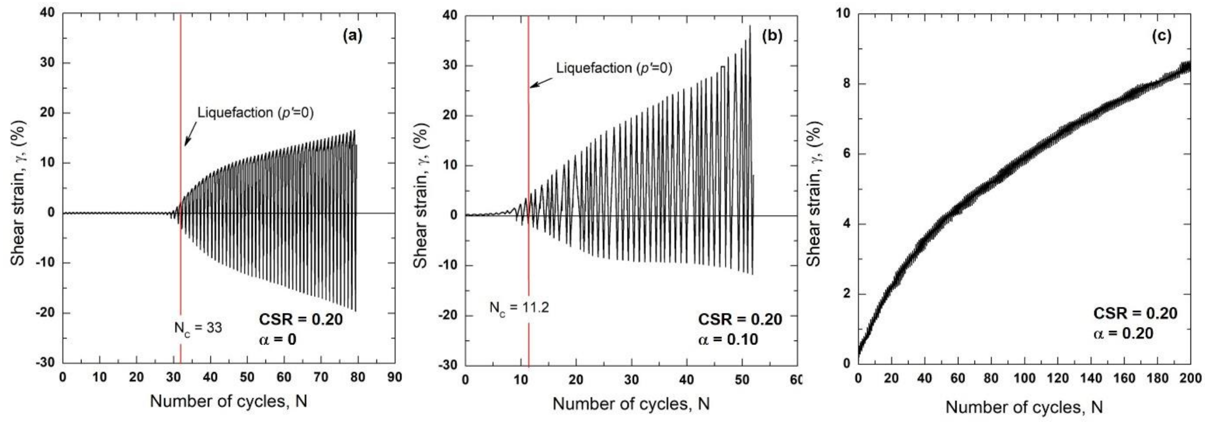

Figure 8. Accumulation of shear strain for CSR=0.20 *CSR* = 0.20 and varying α values

Figure 9 and **Figure 10** shows the comparison of *PWP,* strain accumulation and differential stress variation for α = 0.10 subjected to a *CSR* of 0.20 and 0.30. It can be observed that the number of cyclic decreased from 11.2 to 7 with the increase in the *CSR* from 0.20 to 0.30 to reach the state of *p'*= 0. After liquefaction occurrence (post-liquefaction stage), both the specimens developed large deformation with increasing number of loading cycles. It can be observed from **Figure 9;** the undrained cyclic behavior can be divided into three distinct regions. In the first region, the specimen achieved the state of liquefaction (p'= 0) with a progressive increment in the *PWP* development. The second region is characterized by a sudden development of large strain accumulation at a constant *PWP* increment. The transition from region 2 to 3 takes place by the change in the strain increment and sudden drop of differential stress. Previous studies (Chiaro et al. 2012) reported similar observations for medium dense Toyoura sand subjected to initial static shear.

Furthermore, it can be observed from **Figure 9(c)** and **9(d)**, the transition to region 3 begins at a single amplitude shear strain level of ~14% despite having different *CSR*. Previous studies reported such a cyclic strain accumulation response as the initiation of strain localization in the sandy specimen (Kiyota et al. 2008, Chiaro et al. 2012). The strain at which such transition takes place is termed as limiting strain to initiate strain localization (Kiyota et al., 2008).

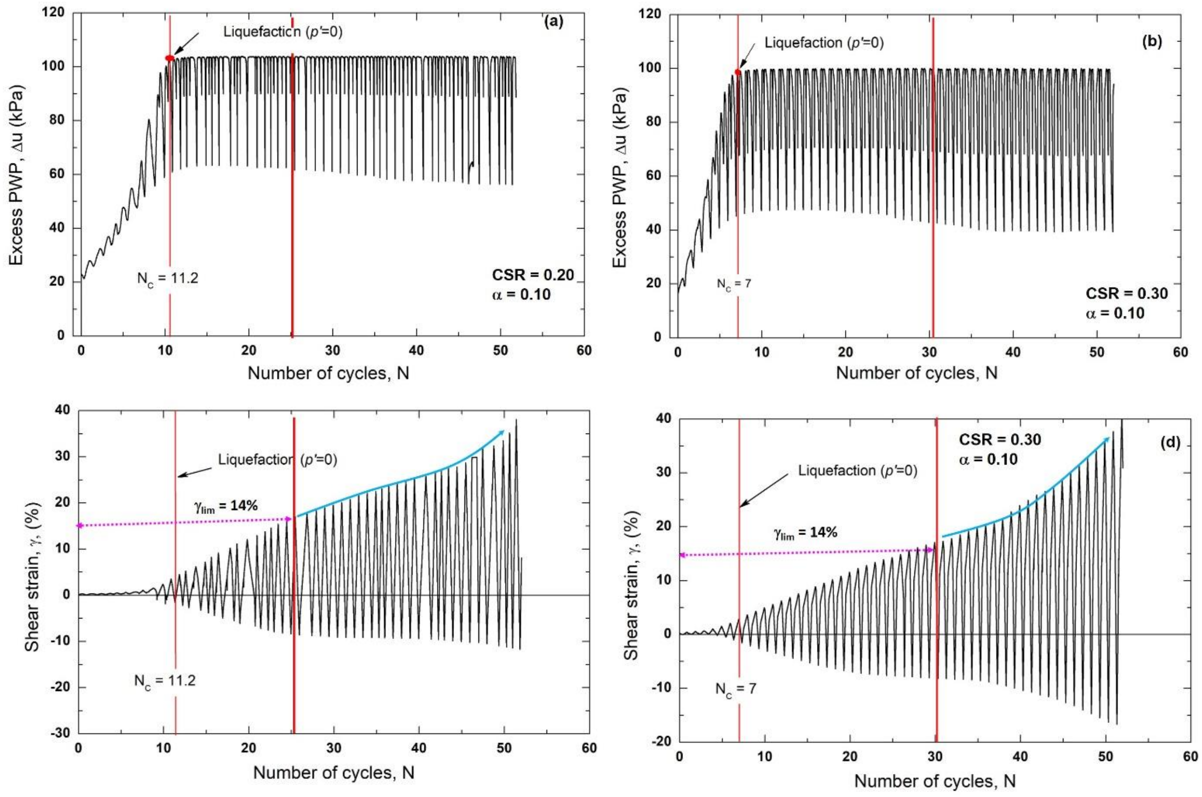

Figure 9. Excess PWP generation and accumulation of shear strain for (a, c) *CSR* = 0.20 and α = 0.10; and (b, d) *CSR* = 0.30 and α = 0.10

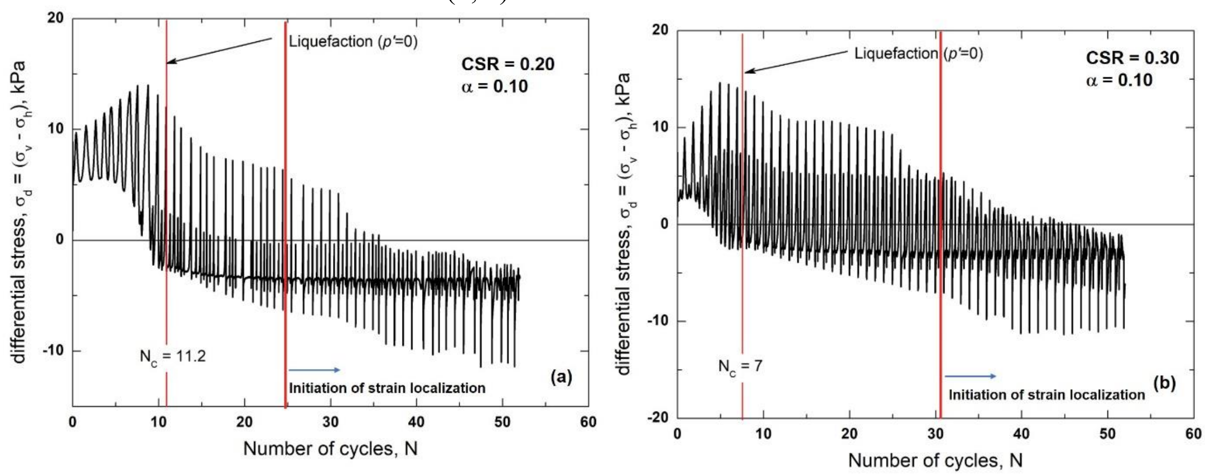

Figure 10. Variation of differential stress against shear strain a) *CSR* = 0.20 and α = 0.10; and (b) *CSR* = 0.30 and α = 0.10

Effects of increasing initial static shear on cyclic resistance

To assess the effect of α on the cyclic shear resistance of the sandy specimen, the applied *CSR* of 0.20 is plotted against the number of loading cycles to reach a single amplitude shear strain (γ_{SA}) of 3.5%, 7.5%, and 15% as shown in **Figure 11**. Experimental results from Chiaro et al. (2012) are also plotted for comparison purposes for medium dense Toyoura sand (D_r = 44-48%) for *CSR* 0.20.

Figure 11 shows that for dense sand, the number of loading cycles to achieve a strain level of γ_{SA} = 3.5%,7.5%, and 15% decreased with the increase in α from 0 to 0.10 and increased for α = 0.20.

The cyclic resistance (γ_{SA} = 7.5%) for level ground condition (α = 0) for the medium dense specimen (D_r ≈ 45%) is lower as compared to the dense specimen (D_r ≈ 71%). Whereas, with the increase in α from 0.05 to 0.20, the cyclic resistance tends to decrease initially and becomes constant.

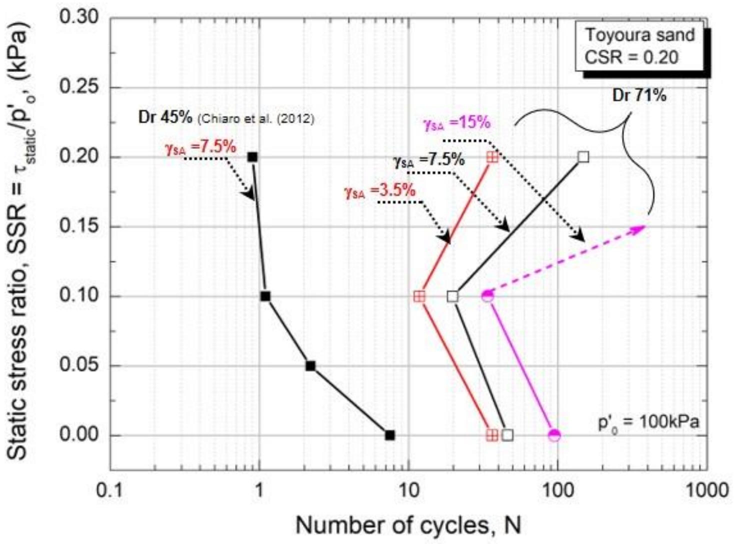

Figure 11. Static stress ratio against number of cycles

CONCLUSIONS

In this paper, the effect of initial static shear on the cyclic undrained behavior of dense Toyoura sand (D_r ≈ 71%) was investigated. Results of torsional simple shear tests revealed that the increase in the initial static shear is detrimental in the stress reversal loading conditions and beneficial in the stress intermediate loading conditions. The cyclic response of dense sand subjected to reversal loading exhibited cyclic mobility in which the specimen developed a progressive buildup of excess pore water pressure and reached the full liquefaction state, which was then followed by a large shear strain accumulation. On the other hand, under intermediate loading full liquefaction was not reached but large residual deformation accumulation occurred, leading to the specimen's failure. The cyclic accumulation resistance of specimens was found to decrease with increasing static stress ratio (α) for stress reversal loading and to increase with increasing α for intermediate loading conditions.

REFERENCES

Chiaro, G., Koseki, J & Sato, T. (2012) "Effects of initial static shear on liquefaction and large deformation properties of loose saturated Toyoura sand in undrained cyclic torsional shear tests." *Soil and foundations* 2012; 52(3):498–510.

Chiaro, G., Kiyota, T. & Koseki, J., (2013) "Strain localization characteristics of loose Toyoura sand in undrained cyclic torsional shear tests with initial static shear.", *Soils and Foundations*, 53(1): 23-34.

Chiaro, G., Umar, M., Kiyota, T., & Koseki, J. (2021) "Deformation and cyclic strength characteristics of sand under sloping ground conditions: insights from cyclic undrained torsional shear tests with static shear." *Geotechnical Engineering Journal of the SEAGS & AGSSEA, Vol. 52, No. 1 (in press).*

Hyodo, M., Murata, H., Yasufuku, N. and Fujii, T. (1991) "Undrained cyclic shear strength and residual shear strain of saturated sand by cyclic triaxial tests", *Soils and Foundations*, 31: 60-76.

Hyodo, M., Tanimizu, H., Yasufuku, N. and Murata, H. (1994) "Undrained cyclic and monotonic triaxial behavior of saturated loose sand." *Soils and Foundations*, 34: 19-32.

Ishihara, K., and Takatsu, H., (1977) "Pore Pressure Buildup in Initially Sheared Sand Subjected to Irregular Excitation." *Proceedings of the 6th World Conference on Earthquake Engineering, New Delhi, India,* 1977, pp. 2163-2168

Kiyota, T., Sato, T., Koseki, J., and Mohammad, A. (2008) "Behavior of liquefied sands under extremely large strain levels in cyclic torsional shear tests." *Soils and Foundations*, 48 (5), 727-739

Koseki, J., Yoshida, T. & Sato, T. (2005) "Liquefaction properties of Toyoura sand in cyclic torsional shear tests under low confining stress." *Soils and Foundations*, 45(5): 103-113

Lee, K. L., and Seed, H. B. (1967) "Dynamic Strength of Anisotropically Consolidated Sand," Journal of the Soil Mechanics and Foundations Division, *ASCE, Vol. 93, No. SM5, 1967, pp. 169-190.*

Tatsuoka, F., Muramatsu, M. and Sasaki, T. (1982) "Cyclic undrained stress-strain behavior of dense sand by torsional simple shear test", *Soils and Foundations, 22 (2), 55-69*

Tatsuoka, F., Sonoda, S., Hara, K., Fukushima S. & Pradhan, T. B. S. (1986) "Failure and deformation of sand in torsional shear." *Soils and Foundations*, 26(4): 79-97.

Towhata, I. 2008: Geotechnical Earthquake Engineering, *Springer*

Umar, M., Chiaro, G., & Kiyota, T. (2016) "On the influence of initial static shear on large deformation behavior of very loose Toyoura sand in undrained cyclic torsional shear tests." *JGS Special Publication*, 4: 17-22.

Umar M., Chiaro G & Kiyota T., (2017) "Influence of density on large deformation characteristic of sand in undrained cyclic torsional shear tests with initial static shear" *In: Proc. of the 3rd International Conference on Performance-based Design in Earthquake Geotechnical Engineering,* Vancouver, Canada, pp. 8.

Vaid, Y. P. and Finn, W.D.L., (1979) "Static shear and liquefaction potential", *Journal of Geotechnical Engineering Division, ASCE,* 105 (GT10), 1233-1246

Vaid, Y. P., and Chern, T.-C, (1983) "Effect of Static Shear on Resistance to Liquefaction." *Soils and Foundations, Japanese Society of Soil Mechanics and Foundation Engineering,* Vol. 23, No. 1, 1983, pp. 47-60.

Vaid, Y.P., Stedman, J.D., Sivathayalan, S., (2001) "Confining stress and static shear effects in cyclic liquefaction", *Canadian Geotechnical Journal,* 38: 580-591.

Yang, J. and Sze, H., 2011: Cyclic Strength of Sand under Sustained Shear Stress." *J. Geotech. Geoenviron. Eng.*, 10.1061/(ASCE)GT.1943-5606.0000541, 1275-1285.

Yoshimi, Y. and Oh-oka, H. (1975) "Influence of degree of shear stress reversal on the liquefaction potential of saturated sand", *Soils and Foundations,* 15 (3), 27-40